Search for $\bar{B}^0 \to \Lambda_c^+ \bar{\Lambda}_c^-$ decay at Belle

Y. Uchida,[5] H. Ozaki,[6] H. Kichimi,[6] I. Adachi,[6] H. Aihara,[7] K. Arinstein,[1] T. Aushev,[8,9] A. M. Bakich,[10] V. Balagura,[9] E. Barberio,[11] A. Bay,[8] K. Belous,[12] V. Bhardwaj,[13] U. Bitenc,[14] A. Bondar,[1] A. Bozek,[15] M. Bračko,[14,16] T. E. Browder,[17] M.-C. Chang,[4] Y. Chao,[18] A. Chen,[19] W. T. Chen,[19] B. G. Cheon,[20] R. Chistov,[9] I.-S. Cho,[21] Y. Choi,[22] J. Dalseno,[11] M. Dash,[23] A. Drutskoy,[3] S. Eidelman,[1] N. Gabyshev,[1] B. Golob,[14,24] H. Ha,[25] J. Haba,[6] K. Hayasaka,[26] M. Hazumi,[6] D. Heffernan,[27] Y. Hoshi,[28] W.-S. Hou,[18] Y. B. Hsiung,[18] H. J. Hyun,[29] K. Ikado,[26] K. Inami,[26] A. Ishikawa,[30] R. Itoh,[6] M. Iwabuchi,[5] M. Iwasaki,[7] Y. Iwasaki,[6] D. H. Kah,[29] H. Kaji,[26] J. H. Kang,[21] N. Katayama,[6] H. Kawai,[2] T. Kawasaki,[31] Y. J. Kim,[5] K. Kinoshita,[3] S. Korpar,[14,16] P. Križan,[14,24] P. Krokovny,[6] C. C. Kuo,[19] A. Kuzmin,[1] Y.-J. Kwon,[21] J. S. Lee,[22] M. J. Lee,[32] S. E. Lee,[32] T. Lesiak,[15] S.-W. Lin,[18] D. Liventsev,[9] F. Mandl,[33] S. McOnie,[10] T. Medvedeva,[9] W. Mitaroff,[33] H. Miyake,[27] H. Miyata,[31] Y. Miyazaki,[26] R. Mizuk,[9] G. R. Moloney,[11] Y. Nagasaka,[34] E. Nakano,[35] M. Nakao,[6] H. Nakazawa,[19] Z. Natkaniec,[15] S. Nishida,[6] O. Nitoh,[36] T. Nozaki,[6] S. Ogawa,[37] T. Ohshima,[26] S. Okuno,[38] S. L. Olsen,[17,39] P. Pakhlov,[9] G. Pakhlova,[9] C. W. Park,[22] H. Park,[29] L. S. Peak,[10] R. Pestotnik,[14] L. E. Piilonen,[23] Y. Sakai,[6] O. Schneider,[8] K. Senyo,[26] M. E. Sevior,[11] M. Shapkin,[12] C. P. Shen,[39] H. Shibuya,[37] J.-G. Shiu,[18] B. Shwartz,[1] J. B. Singh,[13] A. Somov,[3] S. Stanič,[40] M. Starič,[14] T. Sumiyoshi,[41] S. Y. Suzuki,[6] F. Takasaki,[6] M. Tanaka,[6] G. N. Taylor,[11] Y. Teramoto,[35] I. Tikhomirov,[9] K. Ueno,[18] T. Uglov,[9] Y. Unno,[20] S. Uno,[6] P. Urquijo,[11] Y. Usov,[1] G. Varner,[17] K. Vervink,[8] C. C. Wang,[18] C. H. Wang,[42] M.-Z. Wang,[18] P. Wang,[39] Y. Watanabe,[38] R. Wedd,[11] E. Won,[25] Y. Yamashita,[43] M. Yamauchi,[6] C. C. Zhang,[39] Z. P. Zhang,[44] V. Zhulanov,[1] A. Zupanc,[14] and O. Zyukova[1]

(Belle Collaboration)

[1]*Budker Institute of Nuclear Physics, Novosibirsk*
[2]*Chiba University, Chiba*
[3]*University of Cincinnati, Cincinnati, Ohio 45221*
[4]*Department of Physics, Fu Jen Catholic University, Taipei*
[5]*The Graduate University for Advanced Studies, Hayama*
[6]*High Energy Accelerator Research Organization (KEK), Tsukuba*
[7]*Department of Physics, University of Tokyo, Tokyo*
[8]*École Polytechnique Fédérale de Lausanne (EPFL), Lausanne*
[9]*Institute for Theoretical and Experimental Physics, Moscow*
[10]*University of Sydney, Sydney, New South Wales*
[11]*University of Melbourne, School of Physics, Victoria 3010*
[12]*Institute of High Energy Physics, Protvino*
[13]*Panjab University, Chandigarh*
[14]*J. Stefan Institute, Ljubljana*
[15]*H. Niewodniczanski Institute of Nuclear Physics, Krakow*
[16]*University of Maribor, Maribor*
[17]*University of Hawaii, Honolulu, Hawaii 96822*
[18]*Department of Physics, National Taiwan University, Taipei*
[19]*National Central University, Chung-li*
[20]*Hanyang University, Seoul*
[21]*Yonsei University, Seoul*
[22]*Sungkyunkwan University, Suwon*
[23]*Virginia Polytechnic Institute and State University, Blacksburg, Virginia 24061*
[24]*University of Ljubljana, Ljubljana*
[25]*Korea University, Seoul*
[26]*Nagoya University, Nagoya*
[27]*Osaka University, Osaka*
[28]*Tohoku Gakuin University, Tagajo*
[29]*Kyungpook National University, Taegu*
[30]*Saga University, Saga*
[31]*Niigata University, Niigata*
[32]*Seoul National University, Seoul*
[33]*Institute of High Energy Physics, Vienna*
[34]*Hiroshima Institute of Technology, Hiroshima*
[35]*Osaka City University, Osaka*
[36]*Tokyo University of Agriculture and Technology, Tokyo*

[37]*Toho University, Funabashi*
[38]*Kanagawa University, Yokohama*
[39]*Institute of High Energy Physics, Chinese Academy of Sciences, Beijing*
[40]*University of Nova Gorica, Nova Gorica*
[41]*Tokyo Metropolitan University, Tokyo*
[42]*National United University, Miao Li*
[43]*Nippon Dental University, Niigata*
[44]*University of Science and Technology of China, Hefei*

We search for the doubly charmed baryonic decay $\bar{B}^0 \to \Lambda_c^+ \bar{\Lambda}_c^-$, in a data sample of 520×10^6 $B\bar{B}$ events accumulated at the $\Upsilon(4S)$ resonance with the Belle detector at the KEKB asymmetric-energy $e^+ e^-$ collider. We find no significant signal and set an upper limit of $\mathcal{B}(\bar{B}^0 \to \Lambda_c^+ \bar{\Lambda}_c^-) < 6.2 \times 10^{-5}$ at 90% confidence level. The result is significantly below a naive extrapolation from $\mathcal{B}(B^- \to \Xi_c^0 \bar{\Lambda}_c^-)$ assuming a simple Cabibbo-suppression factor of $|V_{cd}/V_{cs}|^2$. The small branching fraction may be attributed to a suppression due to the large momentum of the baryonic decay products, which has been observed in other charmed baryonic two-body B decays.

The large mass of the b quark and the large quark mixing matrix element V_{cb} [1,2] for the $b \to c$ transition lead to a large branching fraction ($\sim 10\%$) [3] for charmed baryonic decays of the B meson. Charmed baryonic decays into four-, three- and two-body final states have already been observed. The measured branching fractions; $\mathcal{B}(\bar{B}^0 \to \Lambda_c^+ \bar{p}\pi^+\pi^-) = (1.12 \pm 0.05 \pm 0.14 \pm 0.29) \times 10^{-3}$ [4], $\mathcal{B}(B^- \to \Lambda_c^+ \bar{p}\pi^-) = (2.01 \pm 0.15 \pm 0.20 \pm 0.52) \times 10^{-4}$ [5] and $\mathcal{B}(\bar{B}^0 \to \Lambda_c^+ \bar{p}) = (2.19^{+0.56}_{-0.49} \pm 0.32 \pm 0.57) \times 10^{-5}$ [6] (also see Refs. [7–10]), point to a hierarchy of branching fractions depending on the multiplicity in the final state [11]. The measurements provide stringent constraints on theoretical models for charmed baryonic decays of the B meson [12–14].

The hierarchy can be understood by large contributions of various intermediate states known in the decays [4–7,10]. The key is to understand quantitatively the decay mechanism of the two-body decays. For example, $\mathcal{B}(B^- \to \Sigma_c(2455)^0 \bar{p}) = (3.7 \pm 0.7 \pm 0.4 \pm 1.0) \times 10^{-5}$ [5] is observed in the three-body decay $B^- \to \Lambda_c^+ \bar{p}\pi^-$, which is comparable to $\mathcal{B}(\bar{B}^0 \to \Lambda_c^+ \bar{p})$. There is an interesting indication of a very large branching fraction $\mathcal{B}(B^- \to \Xi_c^0 \bar{\Lambda}_c^-) = (2.8 - 5.8) \times 10^{-3}$, based on a recent measurement of the product $\mathcal{B}(B^- \to \Xi_c^0 \bar{\Lambda}_c^-) \cdot \mathcal{B}(\Xi_c^0 \to \Xi^- \pi^+) = (4.8^{+1.0}_{-0.9} \pm 1.1 \pm 1.2) \times 10^{-5}$ [15] and theoretical predictions for $\mathcal{B}(\Xi_c^0 \to \Xi^- \pi^+)$ [16]. This branching fraction is quite large in comparison with $\mathcal{B}(\bar{B}^0 \to \Lambda_c^+ \bar{p})$ and does not follow the hierarchy. Figs. 1(a) and 1(b) show quark diagrams relevant for these decays through Cabibbo-favored $b \to cW^-$ transitions with $W^- \to \bar{u}d$ and $W^- \to \bar{c}s$, respectively. Since we naively expect similar branching fractions as $|V_{cb}^* V_{ud}|^2 \sim |V_{cb}^* V_{cs}|^2$, the two-orders of magnitude difference between $\mathcal{B}(B^- \to \Xi_c^0 \bar{\Lambda}_c^-)$ and $\mathcal{B}(\bar{B}^0 \to \Lambda_c^+ \bar{p})$ is a puzzle. It indicates that there is some mechanism to enhance or suppress specific two-body decays. A discussion of a dynamical suppression mechanism, based on the large Q-value in $\bar{B}^0 \to \Lambda_c^+ \bar{p}$ compared to $B^- \to$

$\Xi_c^0 \bar{\Lambda}_c^-$, is given in Ref. [17]. It is important to study various two-body decays to understand charmed baryonic B decays.

In this report, we study the doubly charmed baryonic decay $\bar{B}^0 \to \Lambda_c^+ \bar{\Lambda}_c^-$ as shown in Fig. 1(c). Given the large branching fraction $\mathcal{B}(B^- \to \Xi_c^0 \bar{\Lambda}_c^-)$ relative to $\mathcal{B}(\bar{B}^0 \to \Lambda_c^+ \bar{p})$, we search for the decay $\bar{B}^0 \to \Lambda_c^+ \bar{\Lambda}_c^-$ and compare the result with simple estimates. We expect $\mathcal{B}(\bar{B}^0 \to \Lambda_c^+ \bar{\Lambda}_c^-) = (7.7 \pm 3.0) \times 10^{-7}$ from $\mathcal{B}(\bar{B}^0 \to \Lambda_c^+ \bar{p})$, taking into account the Cabibbo-suppression factor and the phase space factors in two-body decays proportional to the decay momentum in the B rest frame. Alternatively, we expect $\mathcal{B}(\bar{B}^0 \to \Lambda_c^+ \bar{\Lambda}_c^-) = (1.7 - 3.6) \times 10^{-4}$ from $\mathcal{B}(B^- \to \Xi_c^0 \bar{\Lambda}_c^-)$ [18]. Hence, we expect 0.1 and a few tens (21–46) of events, respectively, from these two estimates in our data sample.

This analysis is based on a data sample of 479 fb^{-1}, corresponding to 520×10^6 $B\bar{B}$ events, which were recorded at the $\Upsilon(4S)$ resonance with the Belle detector at the KEKB asymmetric-energy $e^+ e^-$ collider [19].

The Belle detector is a large-solid-angle spectrometer based on a 1.5 Tesla superconducting solenoid magnet. It consists of a three layer silicon vertex detector for the first sample of $152 \times 10^6 B\bar{B}$ pairs, a four layer silicon vertex
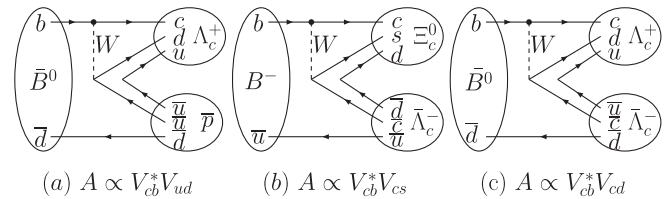

FIG. 1. Quark diagrams for (a) $\bar{B}^0 \to \Lambda_c^+ \bar{p}$, (b) $B^- \to \Xi_c^0 \bar{\Lambda}_c^-$ and (c) $\bar{B}^0 \to \Lambda_c^+ \bar{\Lambda}_c^-$. The first two decays are Cabibbo-favored with Cabibbo-Kobayashi-Maskawa couplings $V_{cb}^* V_{ud}$ and $V_{cb}^* V_{cs}$, respectively, while the third one is Cabibbo-suppressed with coupling $V_{cb}^* V_{cd}$.

detector for the later $368 \times 10^6 B\bar{B}$ pairs, a 50 layer central drift chamber (CDC), an array of aerogel threshold Cherenkov counters (ACC), a barrel-like arrangement of time of flight scintillation counters (TOF), and an electromagnetic calorimeter comprised of CsI(Tl) crystals located inside the superconducting solenoid coil. An iron flux return located outside the coil is instrumented to detect K_L^0 mesons and to identify muons. The detector is described in detail elsewhere [20]. To simulate detector response and to estimate efficiency for signal measurement, we use the Monte Carlo (MC) event generation program EvtGen [21] and a GEANT [22] based detector simulation code.

To search for $\bar{B}^0 \to \Lambda_c^+ \bar{\Lambda}_c^-$ we reconstruct a pair of Λ_c^+'s decaying into $pK^-\pi^+$. Charge-conjugate modes are implicitly included throughout this paper unless noted otherwise. We require tracks to have a distance of closest approach to the interaction point less than 5 cm along the z-axis (opposite to the e^+ beam direction) and 1 cm in a plane perpendicular to the z-axis. Hadrons (protons, kaons and pions) are identified by using likelihood ratios based on CDC dE/dx, TOF and ACC information. We use likelihood ratios $L_s/(L_s + L_b)$, where s and b stand for the hadron species to be identified and for the others, respectively. We require the ratios to be greater than 0.6, 0.6 and 0.4 for proton, kaon and pion selection, respectively. The efficiency for proton identification is 95% with a kaon fake rate of 1.0% due to the small proton momentum ($\sim$ 1 GeV/c) in these baryonic decays. The efficiencies for kaons and pions are about 90%, while the corresponding pion and kaon misidentification rates are approximately 10% [23]. Tracks that are positively identified as electrons or muons are rejected. We impose loose requirements on the vertex fit χ^2's for $\Lambda_c^+ \to pK^-\pi^+ (\chi^2_{\Lambda_c^+})$ and $\bar{B}^0 \to \Lambda_c^+ \bar{\Lambda}_c^- (\chi^2_B)$ to reject background from the decay products of K_S^0 and Λ particles. When there are multiple B candidates (3%) in an event, we choose the candidate with the smallest χ^2_B.

We search for the B signal in the two-dimensional plane of ΔE and M_{bc}. The variable $\Delta E = E_B - E_{beam}$ is the difference between the reconstructed B meson energy (E_B) and the beam energy (E_{beam}). $M_{bc} = \sqrt{E_{beam}^2 - P_B^2}$ is the beam energy constrained B meson mass with the momentum vector of the B meson (P_B). Here E_{beam}, E_B and P_B are defined in the center-of-mass system (CMS). We use the Λ_c^+ mass [3] and the measured momentum of the Λ_c^+ system to calculate E_B, as it gives a better ΔE resolution, 4.3 MeV/c^2, than that calculated with the Λ_c^+ energies reconstructed from the decay products, 6.6 MeV/c^2. To optimize the selection parameters for the signal search, we define a B signal region of $|\Delta E| <$ 0.02 GeV($\sim 4\sigma$) and 5.27 GeV/$c^2 < M_{bc} <$ 5.3 GeV/c^2.

Figure 2 shows the Λ_c^+ mass distribution for (a) data and (b) the MC signal for B signal candidates with $|\Delta E| <$ 0.2 GeV and 5.2 GeV/$c^2 < M_{bc} <$ 5.3 GeV/c^2. We find a significant Λ_c^+ mass peak in the data due to the large inclusive branching fraction for B meson decays with a Λ_c^+ baryon in the final state. The curves show fits using a double Gaussian for the signal and a linear function for the background. We obtain a Λ_c^+ yield of 1281 ± 69 events with a $\chi^2/ndf = 59.4/65$ (67.4%). In the fit to the data, we fix the ratio of $\sigma_{tail}/\sigma_{core}$ to 2.29 and the tail fraction (to the total area) to 0.284; these values are obtained from a fit to the MC signal. The parameters σ_{tail} and σ_{core} are the widths for the tail and core Gaussians, respectively. The fitted masses and σ_{core} are (2285.3 ± 0.2) MeV/c^2 and (3.3 ± 0.2) MeV/c^2 for the data, and (2285.9 ± 0.1) MeV/c^2 and (3.2 ± 0.1) MeV/c^2 for the MC signal. We require that the Λ_c^+ masses lie in the range 2.275 GeV/c^2 to 2.295 GeV/c^2 ($\pm 3\sigma_{core}$). As the MC events are generated using the nominal Λ_c^+ mass [3], this implies a possible small bias in the Λ_c^+ mass measurement, which is taken into account in the systematic error as discussed below.

In this analysis, the Λ_c^+ mass requirements are very effective in suppressing the continuum background ($e^+e^- \to q\bar{q}$, $q = u$, d, s, c). The dominant background is from generic B events. To suppress the background further, we use the variable $\cos\theta_B$, which is the cosine of the angle between the reconstructed B direction and the e^-
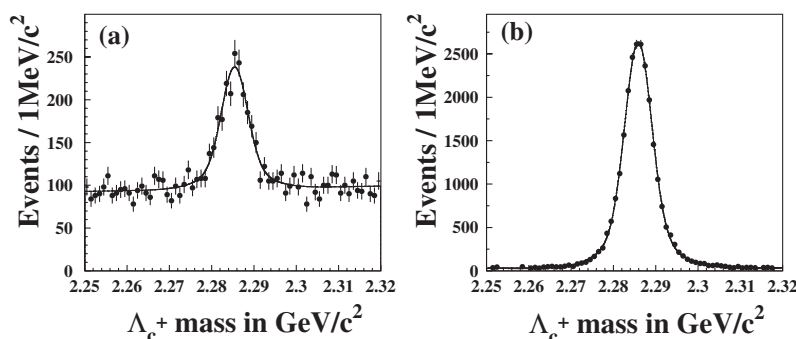

FIG. 2. $\Lambda_c^+(pK^-\pi^+)$ mass distribution for $\bar{B}^0 \to \Lambda_c^+ \bar{\Lambda}_c^-$ candidates in $|\Delta E| <$ 0.2 GeV and 5.2 GeV/$c^2 < M_{bc} <$ 5.3 GeV/c^2. (a) Data and (b) MC signal. The curves show the fits with a double Gaussian for the signal and a linear function for the background.

beam direction in the CMS. The B signal has a $(1 - \cos^2\theta_B)$ distribution while the generic B background and the continuum background have a nearly flat distribution. Using MC simulation, we examine the figure of merit $S/\sqrt{S + N}$ as a function of $\cos\theta_B$. Here, S and N are the signal and background yields in the B signal region, respectively. We assume a branching fraction $\mathcal{B}(\bar{B}^0 \rightarrow \Lambda_c^+ \bar{\Lambda}_c^-) = 5 \times 10^{-5}$ and a sample of 6×10^8 $B\bar{B}$ events, and optimize the figure of merit with the requirement $|\cos\theta_B| < 0.8$.

To obtain the signal yield, we perform an unbinned maximum likelihood fit to the $\bar{B}^0 \rightarrow \Lambda_c^+ \bar{\Lambda}_c^-$ candidates in a two-dimensional (2D) region $-0.15 \text{ GeV} < \Delta E < 0.2 \text{ GeV}$ and $5.2 \text{ GeV}/c^2 < M_{bc} < 5.3 \text{ GeV}/c^2$. We exclude the region $\Delta E < -0.15 \text{ GeV}$, as we find from MC simulation that a background from $B^{-/0} \rightarrow \Lambda_c^+ \bar{\Lambda}_c^- \pi^{-/0}$ populates the region $\Delta E \sim -0.2 \text{ GeV}$. Thus, the effect of the background is negligibly small (< 0.05 events) in the fit region, even if we assume large values of $\mathcal{B}(B^{-/0} \rightarrow \Lambda_c^+ \bar{\Lambda}_c^- K^{-/0})$ [8].

We use a likelihood defined by

$$L = \frac{e^{-(n_s+n_b)}}{n!} \prod_{i=1}^{n} [n_s F_s(\Delta E_i, M_{bci}) + n_b F_b(\Delta E_i, M_{bci})]$$

(1)

with the signal yield n_s and the background yield n_b. The parameter n is the observed number of events. The probability density function (PDF) for the signal $F_s(\Delta E, M_{bc})$ is expressed as a product of a double Gaussian in ΔE and a single Gaussian in M_{bc}, while the PDF for the background $F_b(\Delta E, M_{bc})$ is expressed as a product of a linear function in ΔE and an ARGUS function [24] in M_{bc}.

In the fit, the ΔE and M_{bc} signal shape parameters are fixed to those obtained from one-dimensional fits to the individual simulated distributions for ΔE with $5.27 \text{ GeV}/c^2 < M_{bc} < 5.30 \text{ GeV}/c^2$, and M_{bc} with $|\Delta E| < 0.02 \text{ GeV}$. The yields n_s and n_b, the ΔE linear slope parameter and the ARGUS shape parameter are floated. We obtain a signal efficiency of 0.106 ± 0.001 from a 2D fit to the MC signal. For the fit to the data, we fix the signal parameters to those calibrated for the MC/data systematic difference by using a control sample of $\bar{B}^0 \rightarrow \Lambda_c^+ \bar{p} \pi^+ \pi^-$ decays.

Figure 3 shows the fit to the data. We obtain a signal of $2.7^{+2.7}_{-2.0}$ events with a statistical significance of 1.6σ. The significance is calculated as $\sqrt{-2 \ln(L_0/L_{max})}$, where L_{max} and L_0 are the likelihood values at the fitted signal yield and the signal fixed to zero.

We investigate a possible peaking background in the sideband data, which includes a background from $\bar{B}^0 \rightarrow \Lambda_c^+ \bar{p} \pi^+ \pi^-$ [4], when a π^+ is misidentified as a K^+. We define the sideband by requiring that one of the Λ_c^+ candidate masses lies in the range $2.245 \text{ GeV}/c^2 - 2.325 \text{ GeV}/c^2$ while excluding masses in the range

$2.275 \text{ GeV}/c^2 - 2.295 \text{ GeV}/c^2$. From the 2D fit to the sideband, we estimate a peaking background of -0.1 ± 0.5 events, which is consistent with zero.

We estimate a systematic error of 14.5% in event reconstruction and selection; a 12.6% uncertainty in the efficiency (arising from possible differences between the data and MC simulation in the reconstructed Λ_c^+ mass, particle identification and tracking), a 7.1% uncertainty due to the uncertainty of the signal parameterization used in the 2D fit (obtained by varying the parameters by 1 standard deviation), and a 1.3% uncertainty in the total number of $B\bar{B}$ events. We obtain a total systematic error of 62% in the measured branching fraction, including a 58% uncertainty due to an error in $\mathcal{B}(\Lambda_c^+ \rightarrow pK^-\pi^+) = (5.0 \pm 1.3)\%$ [3] and an 18% error for the peaking background. We correct the signal efficiency by a factor of 0.90 due to a systematic difference in particle identification between MC and data. We assume the same numbers of neutral and charged $B\bar{B}$ pairs, and obtain a branching fraction of $(2.2^{+2.2}_{-1.6}(\text{stat}) \pm 1.3(\text{syst})) \times 10^{-5}$.

We calculate 7.7 events for the upper limit yield at 90% confidence level (CL) by integration of the likelihood function obtained from the 2D fit. We use the formula of $90\% = \int_0^{s_{UL}} L(n|s)ds / \int_0^{\infty} L(n|s)ds$ with $n = 2.7$, where the likelihood $L(n|s) = \int_{-\infty}^{\infty} L_{fit}(n|s^*) \cdot G(s - s^*)ds^*$ is convolved with the Gaussian $G(s - s^*)$ to take into account the total error, which is composed of errors in the fitted yield (the signal and the peaking background), and the systematic error discussed above. The corresponding upper limit is found to be $\mathcal{B}(\bar{B}^0 \rightarrow \Lambda_c^+ \bar{\Lambda}_c^-) < 6.2 \times 10^{-5}$ at 90% CL.

The present result of $\mathcal{B}(\bar{B}^0 \rightarrow \Lambda_c^+ \bar{\Lambda}_c^-) = (2.2^{+2.2}_{-1.6}(\text{stat}) \pm 1.3(\text{syst})) \times 10^{-5}$ is at least 2.6σ smaller than the naive estimate of the range $(1.7 \pm 0.5) - (3.6 \pm 1.1) \times 10^{-4}$ from $\mathcal{B}(B^- \rightarrow \Xi_c^0 \bar{\Lambda}_c^-)$ [15], where the main uncertainty comes from the experimental error in $\mathcal{B}(B^- \rightarrow \Xi_c^0 \bar{\Lambda}_c^-) \cdot \mathcal{B}(\Xi_c^0 \rightarrow \Xi^- \pi^+)$. On the other hand, our limit is consistent with the naive estimate of $(7.7 \pm 3.0) \times 10^{-7}$ from $\mathcal{B}(\bar{B}^0 \rightarrow \Lambda_c^+ \bar{p})$ [6] due to the limited statistics.

Figure 4 compares the result with the data for other charmed baryonic two-body B decays; $B^- \rightarrow \Xi_c^0 \bar{\Lambda}_c^-$, $B^- \rightarrow \Sigma_c(2455)^0 \bar{p}$ [5] and $\bar{B}^0 \rightarrow \Lambda_c^+ \bar{p}$. We define a rescaled branching fraction $\mathcal{F} = \mathcal{B}/(p \cdot \text{CSF})$ [25] to extract a nontrivial component of the decay mechanism. Here p is the decay momentum in the B rest frame, which represents a phase space factor, and CSF is a Cabibbo-suppression factor [3]: 1.0 for $B^- \rightarrow \Xi_c^0 \bar{\Lambda}_c^-$ and $\bar{B}^0 \rightarrow \Lambda_c^+ \bar{p}$, and 0.054 for $\bar{B}^0 \rightarrow \Lambda_c^+ \bar{\Lambda}_c^-$. We also plot $\mathcal{F}(p\bar{p})_{UL}$ for the 90% CL upper limit on $\mathcal{B}(\bar{B}^0 \rightarrow p\bar{p})$ [26] with $\text{CSF} = |V_{ub}/V_{cb}|^2 = 0.011$ [3] assuming a $b \rightarrow u(d\bar{u})$ tree transition. The open and solid points with error bars show the data for B^- and $\bar{B}^0$ decays, respectively. The dashed line shows the function $\ln(\mathcal{F}(p)) = c + s \times p$ with $s = -6.9 \pm 0.8 \text{ (GeV}/c)^{-1}$ to guide the eye, which is obtained by a fit to the three data points. Here, we assume
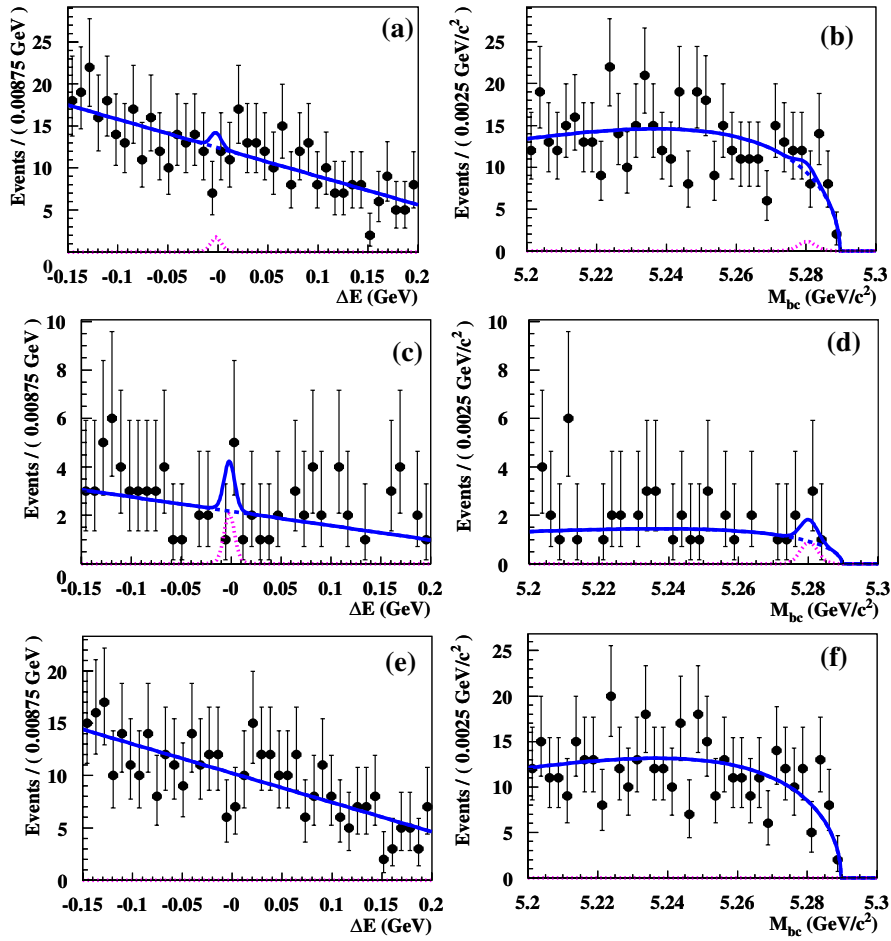
FIG. 3 (color online). Two-dimensional unbinned likelihood fit to the data in -0.15 GeV $< \Delta E < 0.20$ GeV and 5.20 GeV$/c^2 < M_{\rm bc} < 5.30$ GeV$/c^2$. (a) ΔE and (b) $M_{\rm bc}$ distributions for all events. (c) ΔE distribution for 5.27 GeV$/c^2 < M_{\rm bc} < 5.30$ GeV$/c^2$, and (d) $M_{\rm bc}$ distribution for $|\Delta E| < 0.02$ GeV. (e) ΔE distribution for $M_{\rm bc} < 5.27$ GeV$/c^2$ and (f) $M_{\rm bc}$ distribution for $|\Delta E| > 0.02$ GeV. The curves represent the fitted signal (dotted lines) and the total (solid lines) yield.

a simple parametrization, as there is no theoretical prediction for $\ln(\mathcal{F}(p))$. The 90% CL upper limit $\mathcal{F}(\Lambda_c^+ \bar{\Lambda}_c^-)_{\rm UL}$ is close to the extrapolation from the dashed line.

In summary, we search for the doubly charmed baryonic decay $\bar{B}^0 \rightarrow \Lambda_c^+ \bar{\Lambda}_c^-$ in a data sample of 520×10^6 $B\bar{B}$
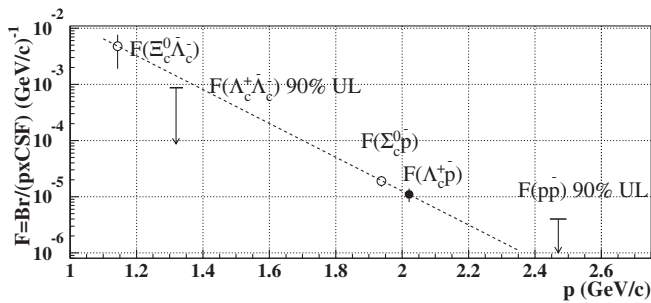

FIG. 4. The rescaled branching fraction $\mathcal{F} = \mathcal{B}/(p \cdot \mathrm{CSF})$ for $B^- \rightarrow \Xi_c^0 \bar{\Lambda}_c^-$, $\bar{B}^0 \rightarrow \Lambda_c^+ \bar{\Lambda}_c^-$, $B^- \rightarrow \Sigma_c^0 \bar{p}$, $\bar{B}^0 \rightarrow \Lambda_c^+ \bar{p}$ and $\bar{B}^0 \rightarrow p\bar{p}$ decays. The dashed line shows a fit to $\ln(\mathcal{F}(p)) = c + s \times p$ with $s = -6.9 \pm 0.8$ $(\mathrm{GeV}/c)^{-1}$ to guide the eye.

events. We obtain $\mathcal{B}(\bar{B}^0 \rightarrow \Lambda_c^+ \bar{\Lambda}_c^-) = (2.2^{+2.2}_{-1.6}(\mathrm{stat}) \pm 1.3(\mathrm{syst})) \times 10^{-5}$ with an upper limit of $\mathcal{B}(\bar{B}^0 \rightarrow \Lambda_c^+ \bar{\Lambda}_c^-) < 6.2 \times 10^{-5}$ at 90% confidence level. The result is significantly smaller than a naive extrapolation from $\mathcal{B}(B^- \rightarrow \Xi_c^0 \bar{\Lambda}_c^-)$, assuming a simple Cabibbo-suppression factor. The suppression of $\bar{B}^0 \rightarrow \Lambda_c^+ \bar{\Lambda}_c^-$ may be attributed to the strong momentum dependence of the decay amplitude that has been observed in other charmed baryonic two-body B decays.

[1] N. Cabibbo, Phys. Rev. Lett. **10**, 531 (1963).

[2] M. Kobayashi and K. Maskawa, Prog. Theor. Phys. **49**, 652 (1973).

[3] W.-M. Yao *et al.* (Particle Data Group), J. Phys. G **33**, 1 (2006).

[4] K. S. Park *et al.* (Belle Collaboration), Phys. Rev. D **75**, 011101 (2007).

[5] N. Gabyshev *et al.* (Belle Collaboration), Phys. Rev. Lett. **97**, 242001 (2006).

[6] N. Gabyshev *et al.* (Belle Collaboration), Phys. Rev. Lett. **90**, 121802 (2003).

[7] N. Gabyshev *et al.* (Belle Collaboration), Phys. Rev. D **66**, 091102(R) (2002).

[8] N. Gabyshev *et al.* (Belle Collaboration), Phys. Rev. Lett. **97**, 202003 (2006).

[9] X. Fu *et al.* (CLEO collaboration), Phys. Rev. Lett. **79**, 3125 (1997).

[10] S. A. Dytman *et al.* (CLEO Collaboration), Phys. Rev. D **66**, 091101(R) (2002).

[11] H. Kichimi (Belle Collaboration), Nucl. Phys. B, Proc. Suppl. **142**, 197 (2005).

[12] M. Jarfi *et al.*, Phys. Lett. B **237**, 513 (1990); Phys. Rev. D **43**, 1599 (1991); N. Deahpande, J. Trampetic, and A. Soni, Mod. Phys. Lett. A **3**, 749 (1988).

[13] V. Chernyak and I. Zhitnisky, Nucl. Phys. **B345**, 137 (1990).

[14] H. Y. Cheng and K. C. Yang, Phys. Rev. D **67**, 034008 (2003).

[15] R. Chistov *et al.* (Belle Collaboration), Phys. Rev. D **74**, 111105(R) (2006).

[16] We estimate $\mathcal{B}(B^- \to \Xi_c^0 \bar{\Lambda}_c^-) = (2.8 \pm 1.1) \times 10^{-3} - (5.8 \pm 2.3) \times 10^{-3}$ and $\mathcal{B}(\bar{B}^0 \to \Xi_c^+ \bar{\Lambda}_c^-) = (0.9 \pm 0.5) \times 10^{-3} - (7.9 \pm 4.1) \times 10^{-3}$ from the measurements [15] of the products $\mathcal{B}(B^- \to \Xi_c^0 \bar{\Lambda}_c^-) \cdot \mathcal{B}(\Xi_c^0 \to \Xi^- \pi^+) = (4.8^{+1.0}_{-0.9} \pm 1.1 \pm 1.2) \times 10^{-5}$ and $\mathcal{B}(\bar{B}^0 \to \Xi_c^+ \bar{\Lambda}_c^-) \cdot \mathcal{B}(\Xi_c^+ \to \Xi^- \pi^+ \pi^+) = (9.3^{+3.7}_{-2.8} \pm 1.9 \pm 2.4) \times 10^{-5}$, respectively. Here, we assume $\mathcal{B}(\Xi_c^0 \to \Xi^- \pi^+) = 0.83\% - 1.74\%$, and $\mathcal{B}(\Xi_c^+ \to \Xi^- \pi^+ \pi^+) = 1.2\% - 10.1\%$ from $\mathcal{B}(\Xi_c^+ \to \Xi^0 \pi^+) = 0.84\% - 3.93\%$, based on theoretical predictions [17,27–30] (see Table. III of Ref [27]) and a measurement of $\mathcal{B}(\Xi_c^+ \to \Xi^0 \pi^+)/\mathcal{B}(\Xi_c^+ \to \Xi^- \pi^+ \pi^+) = 0.55 \pm 0.16$ [3], as they are not measured experimentally. We quote the minimum and maximum estimates to cover the uncertainty in theoretical predictions.

[17] H.-Y. Cheng, C.-K. Chua, and S.-Y. Tsai, Phys. Rev. D **73**, 074015 (2006).

[18] Then, we estimate $\mathcal{B}(\bar{B}^0 \to \Lambda_c^+ \bar{\Lambda}_c^-) = (1.7 \pm 0.5 \pm 0.4) \times 10^{-4} - (3.6 \pm 1.1 \pm 0.9) \times 10^{-4}$ from $\mathcal{B}(B^- \to \Xi_c^0 \bar{\Lambda}_c^-)$, and $(0.58 \pm 0.26 \pm 0.15) \times 10^{-4} - (4.9 \pm 2.2 \pm 0.9) \times 10^{-4}$ from $\mathcal{B}(\bar{B}^0 \to \Xi_c^+ \bar{\Lambda}_c^-)$, by correcting for the phase space factor (p) and the Cabibbo-suppression factor of 5.4\%. The second error is due to a uncertainty of $\mathcal{B}(\Lambda_c^+ \to pK^- \pi^+)$. We cite the estimates from $\mathcal{B}(B^- \to \Xi_c^0 \bar{\Lambda}_c^-)$ in this text, as these give a more restrictive range.

[19] S. Kurokawa and E. Kikutani, Nucl. Instrum. Methods Phys. Res., Sect. A **499**, 1 (2003), and other papers included in this volume.

[20] A. Abashian *et al.* (Belle Collaboration), Nucl. Instrum. Methods Phys. Res., Sect. A **479**, 117 (2002).

[21] D. J. Lange, Nucl. Instrum. Methods Phys. Res., Sect. A **462**, 152 (2001).

[22] R. Brun *et al.*, CERN, Report No. GEANT 3.21, Report No. DD/EE/84-1, 1984.

[23] E. Nakano, Nucl. Instrum. Methods Phys. Res., Sect. A **494**, 402 (2002).

[24] H. Albrecht *et al.* (ARGUS Collaboration), Phys. Lett. B **229**, 304 (1989); **241**, 278 (1990).

[25] For comparison of those data points, we normalize them to the absolute branching fraction $\mathcal{B}(\Lambda_c^+ \to pK^- \pi^+) = 5.0\%$. We calculate the errors for $\mathcal{F}(\Xi_c^0 \bar{\Lambda}_c^-)$, $\mathcal{F}(\Sigma_c^0 \bar{p})$, $\mathcal{F}(\Lambda_c^+ \bar{p})$ excluding the uncertainty from the Λ_c^+ absolute branching fraction as these modes decay to final states with one Λ_c^+. On the other hand, we include the error for $\mathcal{F}(\bar{B}^0 \to \Lambda_c^+ \bar{\Lambda}_c^-)$ as it decays to two Λ_c's. The error in $\mathcal{F}(\Xi_c^0 \bar{\Lambda}_c^-)$ is taken as half of the variation between $\mathcal{B}(\Xi_c^0 \to \Xi^- \pi^+) = 0.83\%$ and 1.74\% for the two most extreme theoretical predictions.

[26] Y.-T. Tsai *et al.* (Belle Collaboration), Phys. Rev. D **75**, 111101(R) (2007).

[27] H.-Y. Cheng and B. Tseng, Phys. Rev. D **48**, 4188 (1993).

[28] J. G. Körner and M. Kramer, Z. Phys. C **55**, 659 (1992).

[29] P. Zenczykowski, Phys. Rev. D **50**, 402 (1994).

[30] Q. P. Xu and A. N. Kamal, Phys. Rev. D **46**, 270 (1992).